International Journal of Pharmaceutics 415 (2011) 62–72

Contents lists available at ScienceDirect

International Journal of Pharmaceutics

journal homepage: www.elsevier.com/locate/ijpharm

Effect of crystallisation conditions and feedstock morphology on the aerosolization performance of micronised salbutamol sulphate

M.H. Shariare*, M. de Matas, P. York

School of Life Sciences, University of Bradford, BD7 1DP, UK

ARTICLE INFO

Article history:
Received 15 February 2011
Received in revised form 17 May 2011
Accepted 18 May 2011
Available online 12 June 2011

Keywords:
Dry powder inhaler
Crystallisation
Particle size reduction
Fine particle fraction
Salbutamol sulphate

ABSTRACT

Salbutamol sulphate (SS) used in dry powder inhalers requires drug particles in the respirable size range of 1–5 μm to achieve a suitable therapeutic effect. The aim of this study was therefore to determine strategies for controlling drug substance characteristics pre and post-crystallisation to facilitate the production of micronised SS with desirable particle attributes for optimal delivery as an inhaled aerosol. SS batches were crystallised using an antisolvent method to produce a range of crystal morphologies. Air jet milling was then used to reduce the size of crystallised SS particles. Starting materials and micronised batches of SS were characterised in the solid state using a range of techniques with subsequent assessment of aerosol properties.

Assessment of the aerodynamic characteristics of micronised SS delivered by DPI (without any carrier) indicated that fine particle fraction and emitted dose as a percentage of the total recovered dose were dependent on the quality attributes of the micronised SS, which were directly linked to the degree of imperfections and the morphology of the crystalline feedstock used in micronisation.

Aerosolization performance of micronised SS can be optimised by manipulation of feedstock characteristics through crystal engineering and through definition of optimal processing conditions for micronisation.

1. Introduction

Salbutamol sulphate is a β_2-sympathomimetic agent used in dry powder inhalers for the treatment of asthma and chronic obstructive pulmonary disease. The desired particle size of salbutamol sulphate to achieve bronchodilation in mild asthmatics is reported to be 2.8 μm (Zanen et al., 1995) due to its propensity to deposit in the proximal airways where it mediates the function of β_2 receptors associated with bronchial smooth muscle. To achieve the desired particle size, salbutamol sulphate is typically processed by micronisation. Spiral air jet mills can produce ultrafine particles (1–10 μm) through impact and attrition forces, where the degree of particle size reduction depends on the milling conditions and material properties (Brodka-Pfeiffer et al., 2003). In reducing the size of particles it has been observed that the energy required for particle fracture depends on the hardness of the feedstock and the type of stress applied to the coarse particles (Brodka-Pfeiffer et al., 2003).

Rumpf (1973) also proposed that particle fracture occurs in three steps—initiation of cracks, growth and acceleration of cracks and branching of cracks at high speeds with subsequent size reduction. Griffith (1920) previously suggested that almost all materials contain cracks, flaws and dislocations. During milling, forces are concentrated into these flaws which assist in initiating crack propagation leading to particle fracture. Irwin (1948) proposed that the resistance of a material to crack extension is determined by the sum of the surface energy and the plastic strain work. He also recognized that for ductile materials the energy required to form a new crack was insignificant compared to the work done during plastic deformation.

De Vegt (2007) showed that pre-existing flaws affect the mechanical properties of materials, which subsequently influence particle fracture during milling. He proposed that particle breakage rate increases with increased flaw density, yet decreases with greater length of flaws.

Though jet-milling demonstrates notable advantages over other milling process including limited metal contamination, easy cleaning and facilitating processing of temperature sensitive materials, previous research in this area has revealed a number of limitations to its use. In studies undertaken by Feeley (1999), micronised salbutamol sulphate showed high dispersive surface free energy

* Corresponding author. Tel.: +44 1274410346; fax: +44 1274410346.
E-mail addresses: m.h.shariare@bradford.ac.uk, mridul_pharmju@yahoo.com (M.H. Shariare).

0378-5173/$ – see front matter © 2011 Elsevier B.V. All rights reserved.
doi:10.1016/j.ijpharm.2011.05.043

Nomenclature

SI units

C	centigrade
g	gram
l	litre
m	metre
mol	mole
s	second
T	temperature

Prefix used with SI units

k	kilo
m	milli
μ	micro

Symbols

min	minutes
θ	angle of X-ray beam diffraction
$CHCl_3$	chloroform

Abbreviations

SS	salbutamol sulphate
DPI	dry powder inhaler
FPF	fine particle fraction
FPD	fine particle dose
ED	emitted dose
RD	recovered dose
API	active pharmaceutical ingredients
IPA	iso-propyl alcohol
rpm	rotation per minute
IP	injector pressure
GP	grinding pressure
FR	feed rate
RH	relative humidity
SEM	scanning electron microscopy
DSC	differential scanning calorimetry
PXRD	powder X-ray diffractometry
DVS	dynamic vapour sorption
IGC	inverse gas chromatography
TSLI	twin stage liquid impinger
HPMC	hydroxy propyl methyl cellulose
UV	ultraviolet
BCF	Barton, Cabrera and Frank crystal growth model
VMD	volume mean diameter
PDI	polydispersity index
Mag	magnification
UK	United Kingdom

(64.54 mJ/m^2) compared to batches manufactured using a supercritical fluid technique (SEDS) (38.45 mJ/m^2). The micronised material subsequently showed poor flow and low fine particle fraction following aerosolization from a dry powder inhaler. French et al. (1996) suggested that micronisation leads to small and flat particles with large surface area, which increases cohesive and adhesive interactions with adverse consequences for powder handling, flow and aerosolization. Price and Young (2004) observed that strong cohesive forces caused by high surface free energy of micronised materials enhance agglomerate formation, leading to negative effects with regard to the fluidization and dispersion characteristics of inhaler formulations. It was also suggested that the degree of de-agglomeration in these powders is a function of agglomerate cohesive strength, which may directly influence the aerosol characteristics and deposition behaviour of these systems. It is therefore necessary to control the production of active pharmaceutical ingredients (API) used in respiratory products to provide favourable particle and surface characteristics for optimal aerosolization.

The aim of this work detailed in this paper was to determine strategies for controlling the feedstock characteristics of a model API to facilitate the production of a micronised drug with desirable particle attributes for optimal delivery as an inhaled aerosol. Owing to its wide use as a bronchodilator, salbutamol sulphate (SS) was chosen as a model compound in this study. The principal aim was to generate an understanding of the impact of the crystallisation conditions on the morphology of SS crystals and their influence on the quality attributes of micronised powders.

2. Materials and methods

2.1. Materials

Salbutamol sulphate was supplied by Cipla, India (Batch No. H80142). Two batches of micronised salbutamol sulphate were supplied by two generic suppliers (A and B). All solvents used in this study were of analytical grade and were supplied by Sigma–Aldrich, UK except for tetrahydrofuran which was supplied by Rathburn Chemicals Ltd., UK. All compressed gases were supplied by BOC Ltd., Surrey, UK.

2.2. Methods

2.2.1. Crystallisation of SS

Three batches of salbutamol sulphate (SS1, SS2 and SS3) were crystallised using a cosolvent mixture of water and isopropyl alcohol (IPA). Salbutamol sulphate (SS1 and SS2) was dissolved in water (1:5 w/v) at 25 °C with stirring, the solution was then heated from 25 °C to 50 °C at a rate of 0.80 °C/min in a glass jacketed vessel, where the temperature was controlled using a chiller unit (Julabo PF929, Julabo, Germany) (Figure 4.1). IPA was then added at a rate of 90 ml/min using a burette until the IPA: water solvent ratio was 75:25 (v/v) and heated at 50 °C for 30 min. Solutions were then cooled to 25 °C at a rate of 0.14 °C/min. As increase or decrease in temperature over this range did not show any notable influence on the solubility of SS in this study, IPA was therefore added as an antisolvent during SS crystallisation. For SS1 and SS2 the stirring rates were 300 rpm and 400 rpm, respectively (Table 1). SS3 was crystallised using an identical concentration of salbutamol sulphate in water at 25 °C, with IPA added at a rate of 90 ml/min until the solvent ratio was 75:25 (v/v). The sample was then cooled to 10 °C at a rate of 1 °C/min and stored at 10 °C for 24 h.

Crystallised samples were filtered using Whatman qualitative 1 filter paper (55 mm, Whatman International Ltd., England) with the aid of a vacuum pump. Filtered samples were then collected and dried at room temperature for 2–3 days.

2.2.2. Sieving

Dried SS samples with different morphology were then classified into sieve fractions (<20 μm and 50–250 μm) using a set of sieves and associated sieve shaker (Retsch, UK).

2.2.3. Micronisation

Following controlled crystallisation and sieving of the samples, the micronisation behaviour for the different batches (SS1, SS2 and SS3) of salbutamol sulphate was evaluated using the FPS Spiral Jetmill (FPS, Italy). The influence of IP = injector pressure and FR = feed rate at constant grinding pressure (GP) (5 bar) on the quality attributes of micronised powder was evaluated. The levels defined for each of the process parameters are given in Table 2. For

Table 1
Crystallisation conditions used for salbutamol sulphate.

Batch	Salbutamol sulphate concentration (g/ml)	Temperature of IPA addition (°C)	Cooling rate (°C/min)	Duration at 25 °C (h)	Stirring rate (rpm)	Stirring duration (h)
SS1	0.2	50	0.14	24	300	25
SS2	0.2	50	0.14	24	400	25
SS3	0.2	25	1.0	1.30	300	2

each experiment, a 5 g sample of each batch of salbutamol sulphate was processed.

For SS1, SS2 and SS3, two different sieve fractions (50–250 μm and <20 μm) were micronised to evaluate the impact of particle size on the quality of size reduced salbutamol sulphate. Feed rates were determined using samples at the highest and lowest settings of the speed controller obtained from screening experiments conducted in triplicate. Powder was collected at 1 min intervals and the weight determined using a standard balance. Grinding and injector pressures were set using the appropriate regulator with the pressure display calibrated using an external pressure gauge (accuracy ±1.6%).

Injector pressure, grinding pressure and feed rate were adjusted to provide the conditions stated in Table 2. Samples were collected from the collection vessel at the end of the experiments and stored over phosphorous pentoxide to avoid moisture mediated transformation before characterisation. For all experiments, the moisture content of supplied compressed air was 2–6% RH, which was determined using a hand held hygrometer (Testo 610, Testo, UK).

2.2.4. Molecular modelling

The single crystal structure data for salbutamol sulphate was acquired from the Cambridge Structural Database (CSD, UK) (Allen, 2002). Materials Studio 4.1 (Accelrys, Inc.) was then used for molecular modelling. Geometry optimisations on the crystal structure were performed using the CVFF (with force field assigned charges) and Dreiding (with Qeq and Gasteiger charges) force fields. Morphology calculations were carried out using the BFDH method and the growth morphology method. The BFDH method was used to generate a list of possible growth faces, associated d-spacings and relative facet areas. The growth morphology method was used to calculate the attachment energies of different faces.

2.2.5. Scanning electron microscopy (SEM)

Scanning electron microscopy analysis was carried out for starting and micronised samples using the Quanta 400 SEM (FEI Company, Cambridge, UK). Samples were analysed at a variety of magnifications with direct data capture of the images onto a personal computer. Calibration of the SEM was performed using a gold grid standard supplied with the instrumentation.

2.2.6. Particle size analysis

The particle size distribution was determined for the starting material and processed samples using a laser diffraction particle size analyser (HELOS & RODOS, Sympatec Instruments, UK). 15–20 mg samples were fed into the analyser by ASPIROS unit, using an air pressure of both 4 and 1 bar, at a speed of 30 mm/s. The trigger condition used for both starting and micronised batches was 5 s at an optical concentration of 1%. All samples were analysed in triplicate. Calibration of particle size analyser was performed using a standard silica sample.

2.2.7. Differential scanning calorimetry (DSC)

Thermal properties of the starting material and processed samples were determined using the DSC module of the TA Instruments Q2000 series thermal analysis system (TA Instruments, West Sussex, UK). Samples (1–5 mg) were analysed in a pierced and crimped aluminium pans, with heating under a stream of nitrogen gas from 25 to 250 °C at a scanning rate of 10 °C/min. All samples were analysed in triplicate. The temperature scale was calibrated using a pure indium standard (melting point 156.6 °C) and confirmed using a zinc standard (melting point 419.5 °C).

2.2.8. Powder X-ray diffraction (PXRD)

Powder X-ray diffraction was used to characterise the solid form of samples. Analysis of samples was carried out using a Bruker D-8 powder diffractometer (Bruker, Kahlsruhl, Germany) at room temperature. Samples were placed into plastic sample holder with zero background and levelled using a glass cover slide. Samples were scanned over 5–50° 2θ at a rate of 1° 2θ/min using a copper Kα radiation source of wavelength 1.542 Å with 1 mm slits. Calibration of the PXRD was performed using a carborundum (silicon carbide) standard.

2.2.9. Dynamic vapour sorption (DVS)

Moisture sorption isotherms were determined using a microprocessor controlled automated IGAsorp moisture sorption

Table 2
Sample code for the micronised batches of SS with different morphology.

Starting SS	Micronised sample code	Starting materials particle size (μm)	Process variables		
			GP (bar)	IP (bar)	FR (g/min ± SD[a])
SS1	SS1-1	50–250	5	8	2.50 ± 0.40
	SS1-2	<20	5	8	0.90 ± 0.15
	SS1-3	50–250	5	8	0.42 ± 0.06
SS2	SS2-1	50–250	5	8	3.20 ± 0.50
	SS2-2	<20	5	8	1.30 ± 0.30
	SS2-3	50–250	5	8	0.55 ± 0.10
SS3	SS3-1	50–250	5	8	1.70 ± 0.35
	SS3-2	<20	5	8	1.00 ± 0.20
	SS3-3	50–250	5	8	0.25 ± 0.04

[a] SD: standard deviation.

analyser (IGA*SORP*, Hiden Isochema Ltd., Warrington, UK). Measurements were performed using 30–50 mg of samples at 25 °C, under a continuous nitrogen flow of 250 ml/min in the range of 0–95% RH. Relative humidity was held at each point until equilibrium was achieved. The sample mass was represented as a percentage of the initial mass. Calibration curves for percentage of moisture uptake were constructed using mixture of crystalline and amorphous standards at levels of 1, 3, 5, 10, 25 and 50% (w/w). The amorphous standard was produced by freeze drying a 10% aqueous solution of salbutamol sulphate, which was confirmed by PXRD and DSC analysis. The starting materials for each of the respective sieved batches were used as the crystalline standards. Relative (%) crystallinity of micronised samples was determined from the regression equation for the lines of best fit for each calibration curve.

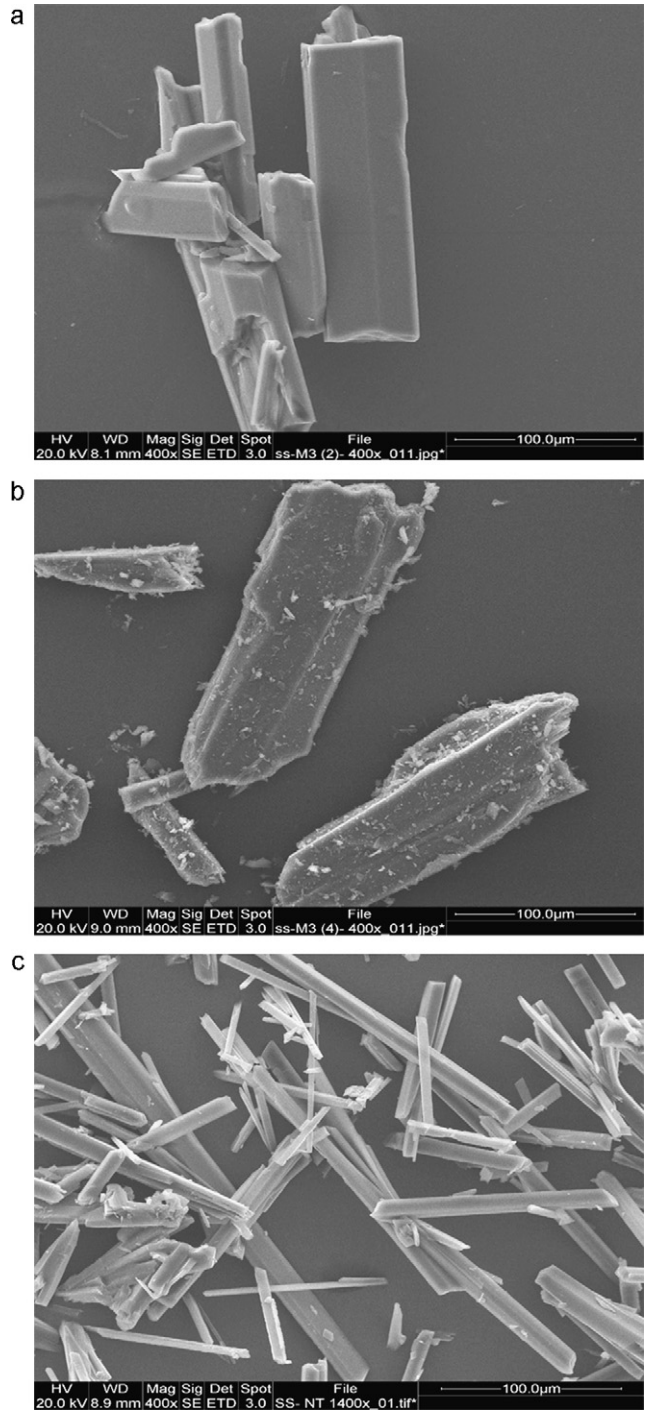

Fig. 1. SEM photographs of three salbutamol sulphate batches: (a) SS1, (b) SS2 and (c) SS3, respectively.

2.2.10. Inverse gas chromatography (IGC)

IGC measurements were carried out using the automated Perkin Elmer gas chromatograph (Perkin Elmer, USA) equipped with a flame ionization detector (FID). Nitrogen was used as carrier gas with hydrogen and compressed air employed for the FID. The flow rate of carrier gas at column outlet (N_{flo}) was measured using a bubble flow meter. The method used in this study has previously been reported by Saxena (2007). The dispersive component surface free energy and specific surface free energy were determined using the method described by Schultz and Lavielle (1989).

2.2.11. Twin stage liquid impinger (TSLI)

A coarse classification of aerodynamic particle size for salbutamol sulphate was determined using a twin stage liquid impinger at 90 l/min delivered from an Aerolizer DPI device (Aerolizer®, Novartis, UK) (Figure 5.1). HPMC capsules (Qualicaps, Spain) (size 3) were filled with 15 ± 1 mg salbutamol sulphate in the absence of any carrier. Methanol and water in a ratio of (50:50) were used as a solvent, with 7 ml and 30 ml introduced into the upper and lower stages of a twin stage liquid impinger (British Pharmacopaeia, 2008), respectively.

The capsule to be tested was placed in the inhaler device, which had been fitted into a moulded rubber mouthpiece attached to the throat of the impinger. Once the assembly had been checked and found to be airtight and vertical, the pump was switched on and the dose released by activating the device. The impinge pump was allowed to run for 2.7 s at 90 l/min before switching off. The test was carried out in triplicate and salbutamol levels were determined using UV analysis at a wavelength of 276 nm. The recovered dose (RD) was the sum of the weights of drug (mg) recovered from the capsule shell, the inhaler device, throat, the upper and lower stages of the twin stage impinger. The emitted dose (ED) was the dose emitted from the inhaler device, depositing in the throat, upper and lower stages of the twin stage impinger. The percentage of emitted dose was calculated with respect to the total recovered dose (RD). Fine particle dose (FPD) was the amount of drug recovered from the lower stage of the impinger, with the fine particle fraction % (FPF) being calculated as a percentage of RD. The aerodynamic characteristics for batches micronised from each of the crystallised samples (SS1, SS2 and SS3) were compared with two micronised salbutamol sulphate samples from generic suppliers.

2.2.12. UV analysis

Salbutamol sulphate samples collected from each stage of twin stage impinger, ACI, device and emptied capsule shell were analysed using UV-Vis spectrophotometer (Jasco V-530, Jasco Ltd., UK) at 276 nm. Methanol:water at a ratio of 50:50 (v/v) used during in vitro study was also used as a blank in this study. The concentration of salbutamol sulphate at different stages was determined from the regression equation for the lines of best fit for calibration curve constructed from a range of standard concentrations (5, 10, 20, 30, 40, 50 and 100 μg/ml).

3. Results and discussion

3.1. Crystallisation

3.1.1. Effect of cooling and stirring rate on the morphology of SS

The SEM photomicrographs (Fig. 1a) show that SS crystallised at slow cooling rates (0.14 °C/min) produced plate like crystals (SS1). The faster stirring rates (400 rpm) used for SS2 gave rise to distorted

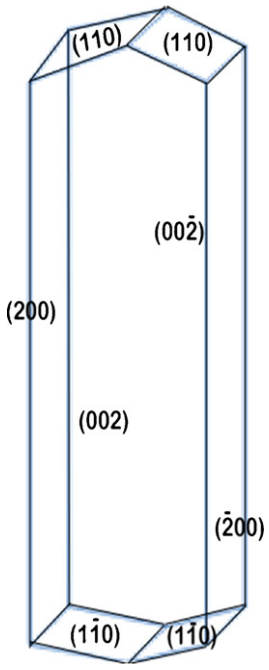

Fig. 2. Predicted major habit faces of salbutamol sulphate crystals (after Feeley, 1999).

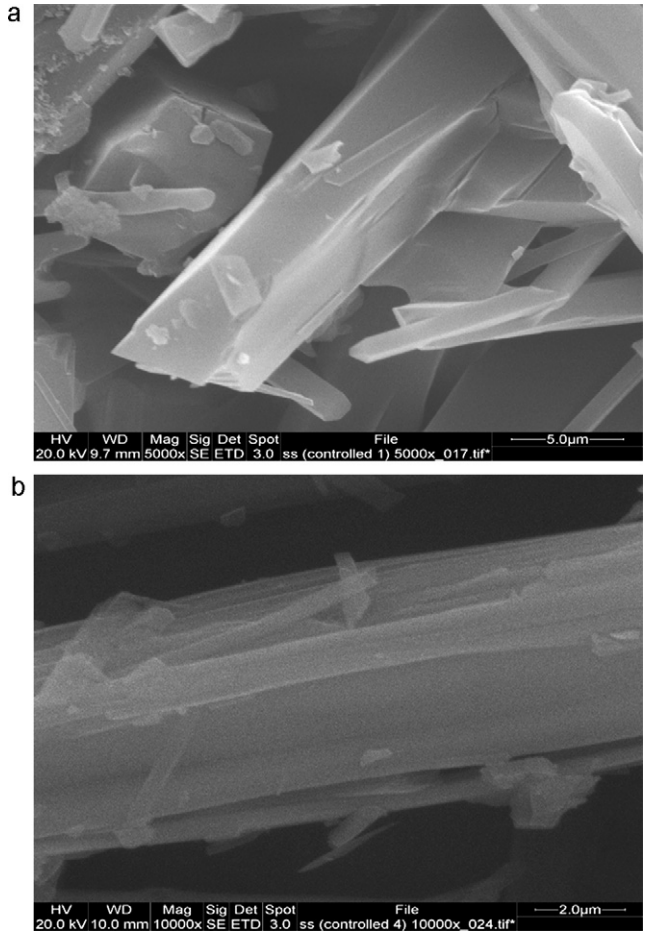

Fig. 3. SEM photomicrographs showing (a) cracks (mag. 5000×) and (b) defects (mag. 10,000×) for SS2 crystals, respectively.

plate like crystals with angular faces with higher density of dislocations and defects (Fig. 1b). SS crystallised at a faster cooling rate (1 °C/min) produced needle like crystals (SS3) (Fig. 1c).

At slower cooling rates, the level of supersaturation is low, where smooth surfaces with sequential layer growth occur (Blagden, 2004). In these experiments, growth has most likely occurred via the (0 0 $\bar{2}$) faces for SS1 (Fig. 2), which has resulted in crystals with plate like morphology and the ($\bar{2}$ 0 0) face being the probable major habit face for these crystals (Figs. 2 and 4). It was however observed that increases of stirring rate and the duration of stirring produced crystals with greater density of dislocations and defects (SS2) (Fig. 3a and b).

This is attributed to the initiation of secondary nucleation and decreased size of the diffusion layer at high stirring rates (Storey, 1997), for which the delivery rate of growth units increases. This phenomenon may lead to difficulties in incorporation of growth units into the crystal lattice which facilitates changes in growth mechanism (BCF mechanism with spiral growth) with consequences for the morphology produced. Salbutamol sulphate crystallised at a faster cooling rate (1 °C/min) produced needle like crystals (SS3), for which growth has most likely occurred via both the (0 0 $\bar{2}$) and ($\bar{2}$ 0 0) faces (Fig. 2). This finding is attributed to the faster cooling rates causing a relatively higher supersaturation (moderate supersaturation) leading to surface nucleation and subsequent growth of SS crystals by the birth and spread mechanism (Ludlam-brown, 1991).

3.1.2. *Effect of crystallisation conditions on solid surface chemistry*

IGC and DVS data obtained are consistent with the observations of the morphological differences for crystallised SS samples with similar particle size distributions (Table 3). SS2 and SS3 clearly demonstrate higher values of dispersive surface free energy compared to SS1 crystals. This phenomenon is related to the high percentage of facet area of the (0 0 $\bar{2}$) face with multitude exposure of the hydrophobic trimethyl groups (Fig. 4b) and greater density of crystal defects for SS2 crystals. DVS data also support these arguments with the lower magnitude of moisture sorption for these materials related to the (0 0 $\bar{2}$) face being the major habit face with trimethyl groups exposed at the surface (Fig. 4b). Conversely, the relatively high moisture level adsorbed by SS1 crystals is primarily ascribed to the ($\bar{2}$ 0 0) face (Fig. 4a), for which sulphate groups are exposed at the surface.

IGC data (Table 3) showed a higher value of specific surface free energy measured using $CHCl_3$ for the SS1 crystals compared to SS2 and SS3. This is attributed to the large number electron donating oxygen of sulphate group ($\bar{2}$ 0 0) behaving in a more electron donating and interacting strongly with the acidic probe chloroform (electron acceptor).

Table 3
Moisture adsorption and surface free energy data of starting material SS1, SS2 and SS3 (value in brackets indicate range value, where $n = 2$).

Samples	% moisture sorption at 95% RH	Dispersive surface energy (mJ/m^2)	Specific surface energy measured using $CHCl_3$ (kJ/mol)
SS1	0.48 (0.05)	34.13 (1.14)	2.33 (0.35)
SS2	0.22 (0.02)	47.02 (3.90)	1.35 (0.17)
SS3	0.20 (0.01)	41.22 (1.61)	1.44 (0.23)

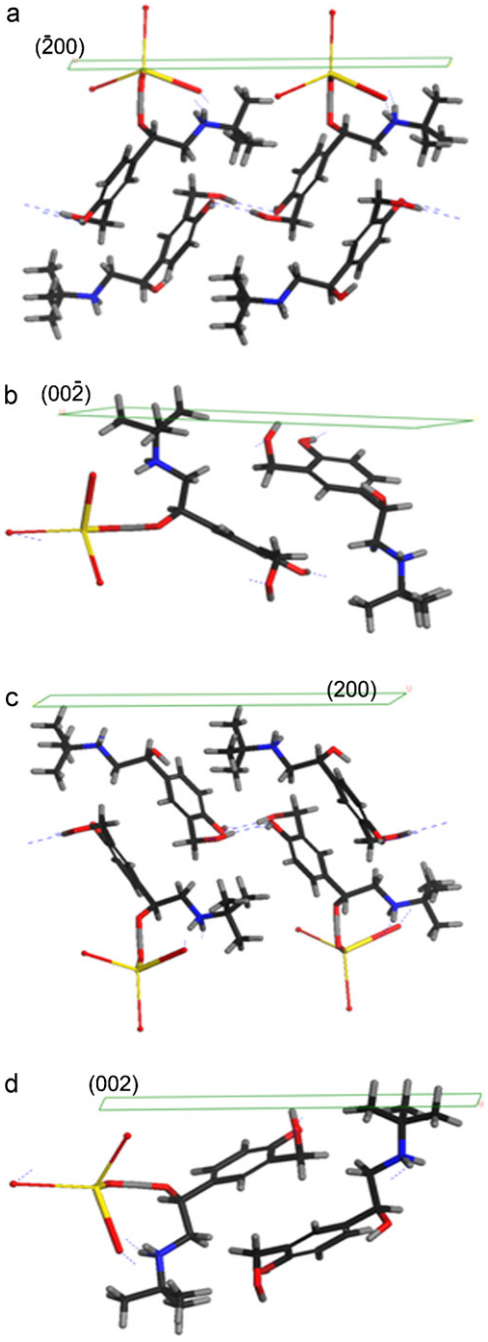

Fig. 4. Molecular orientation of the main crystal faces of salbutamol sulphate.

3.2. Thermal and structural analysis

DSC data, with an endothermic transition for all samples at ~200 °C, demonstrate melting with decomposition for salbutamol sulphate (Ticehurst, 1995). DSC data also showed no notable changes in thermal behaviour between the starting materials and micronised SS powders (Fig. 5).

No polymorphic or solid state conversions were revealed by PXRD between starting and micronised batches of SS1 and SS3. The theoretical PXRD pattern of SS generated from single crystal data (Cambridge Structural Database, UK) using Mercury (version 2.3) (Mercury software package, CCDC, Cambridge, UK) shown in Fig. 6 is consistent with the data observed for SS1 and SS3. However, batches micronised from SS2 (SS2-1) (see Table 2) showed diffuse PXRD scatter below 18° 2θ angles (Fig. 7), which is most likely related to the defects (amorphous content) generated mainly on the (2 0 0) and (0 0 2) faces (Figs. 6 and 7) of SS crystals.

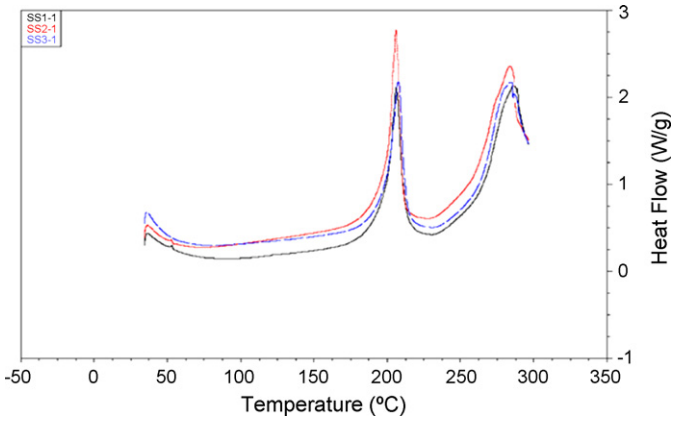

Fig. 5. DSC data for the micronised batches of SS1, SS2 and SS3.

3.3. Particle size analysis

Particle size distribution data, shown in Table 4, demonstrate that batches micronised from SS3 (Fig. 8) showed lower volume mean diameter (μm) and polydispersity compared to batches micronised from the other two starting materials (SS1 and SS2) when using similar grinding pressure, injector pressure and particle size distributions of the feedstock (Table 2). This is thought to be related to the high aspect ratio of needle like SS3 crystals for which the crack propagation length could decrease markedly (De Vegt, 2007). However it is also possible to produce ultrafine material using SS1 and SS2 starting materials (Table 4). Table 2 shows a minor difference in FR between SS1, SS2 and SS3 larger sized starting materials (50–250 μm), which is thought to have an impact on the propensity for particle size reduction (Table 4). However the small sized SS1, SS2 and SS3 (<20 μm) fractions did not show any notable difference between their FR, which indicates that morphology of SS crystals have marked influence on the magnitude of particle size reduction. The level of effect of FR on particle size reduction for the different morphology of SS is further evaluated in Fig. 9.

The particle size of the feedstock has a marked effect on comminution and suggests that batches micronised from finer sized starting material (SS1-2, SS2-2 and SS3-2) typically exhibit lower VMD (Table 4) compared to batches micronised from larger

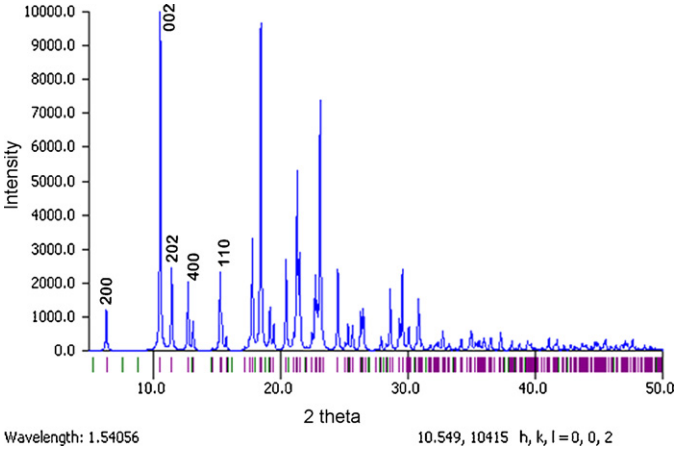

Fig. 6. Theoritical PXRD pattern for salbutamol sulphate.

Table 4
Particle size distribution data for micronised batches of SS1, SS2 and SS3 (values in bracket indicate standard deviation).

Sample	D10 (μm)	D50 (μm)	D90 (μm)	PDI	VMD (μm) at 4 bar
SS1-1	0.73 (0.01)	2.23 (0.02)	5.64 (0.02)	2.10 (0.01)	2.68 (0.07)
SS1-2	0.60 (0.01)	1.65 (0.02)	3.72 (0.02)	1.85 (0.01)	1.93 (0.03)
SS2-1	0.64 (0.03)	2.27 (0.02)	5.40 (0.04)	2.31 (0.05)	2.73 (0.05)
SS2-2	0.62 (0.01)	1.69 (0.02)	3.72 (0.01)	1.83 (0.01)	1.98 (0.04)
SS3-1	0.70 (0.02)	1.95 (0.02)	4.18 (0.03)	1.78 (0.02)	2.03 (0.02)
SS3-2	0.60 (0.01)	1.50 (0.01)	3.43 (0.02)	1.79 (0.02)	1.80 (0.01)

sized starting material when using similar processing conditions. However, this impact of feedstock particle size is morphology dependent and appears to be greater for SS1 and SS2 than the SS3 needle like crystals.

This finding is explained by referring to the high aspect ratio of SS3 crystals, which have the propensity to reorient along the long axis and so may pass through the 20 μm mesh during sieving. The apparent particle size of the needle like crystals (SS3) may therefore bias the effect of particle size on size reduction for SS3. Results also suggest that a high reduction ratio (ratio of initial median particle size to the micronised median particle size) was obtained for coarser grade starting materials. Vogel and Peukert (2003) observed that when applying a similar level of energy, smaller particles exhibit a smaller breakage probability due to the smaller particle contact area containing fewer crystallographic flaws, providing reduced potential for particle fracture.

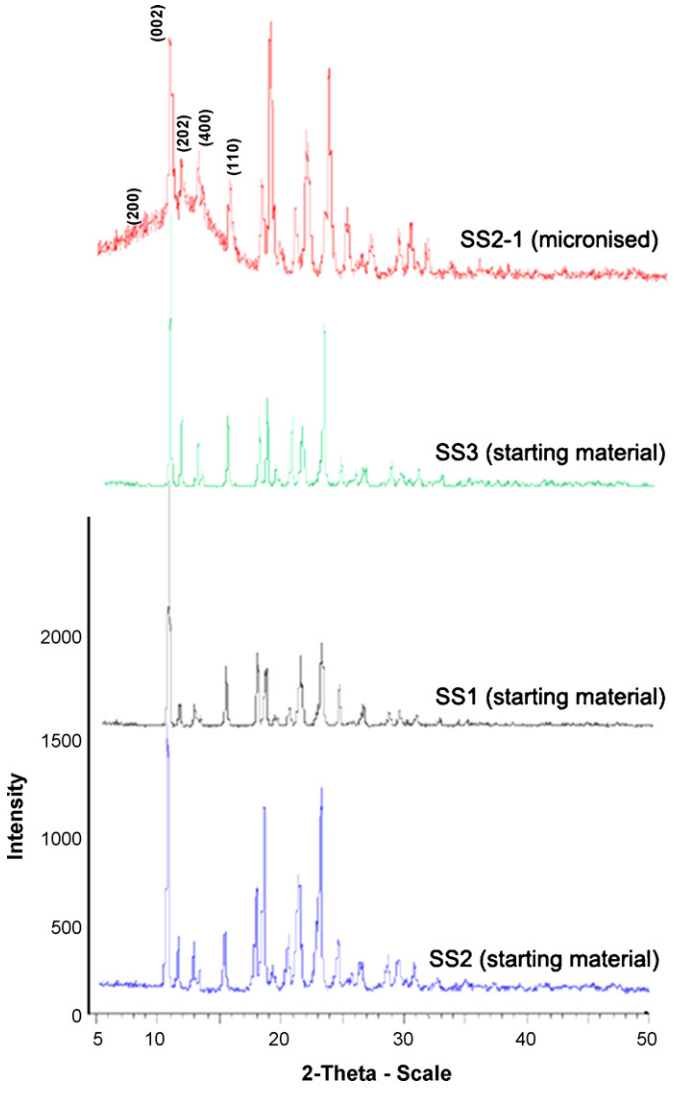

Fig. 7. PXRD data for the starting materials SS1, SS2, SS3 and micronised SS2-1.

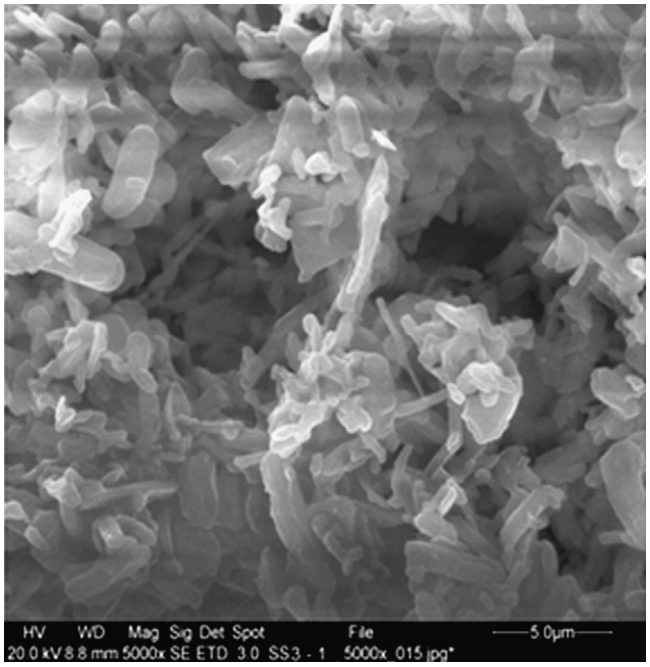

Fig. 8. SEM photomicrographs of micronised SS3-1 (mag. 5000×).

Evaluation of the impact of process conditions on the micronisation of the SS powder with different morphologies has revealed a number of important effects. The feed rate at which the feedstock is delivered to the microniser has been shown to have marked effect on particle size reduction (Fig. 9). This observation indicates that increases in feed rate will lead to a greater degree of particle size reduction for SS crystals, due to larger numbers of particles in the

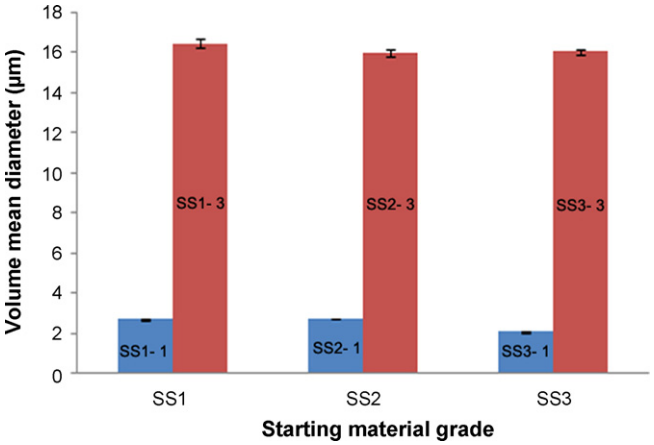

Fig. 9. Effect of feed rate on volume mean diameter observed for micronised batches of SS1, SS2 and SS3.

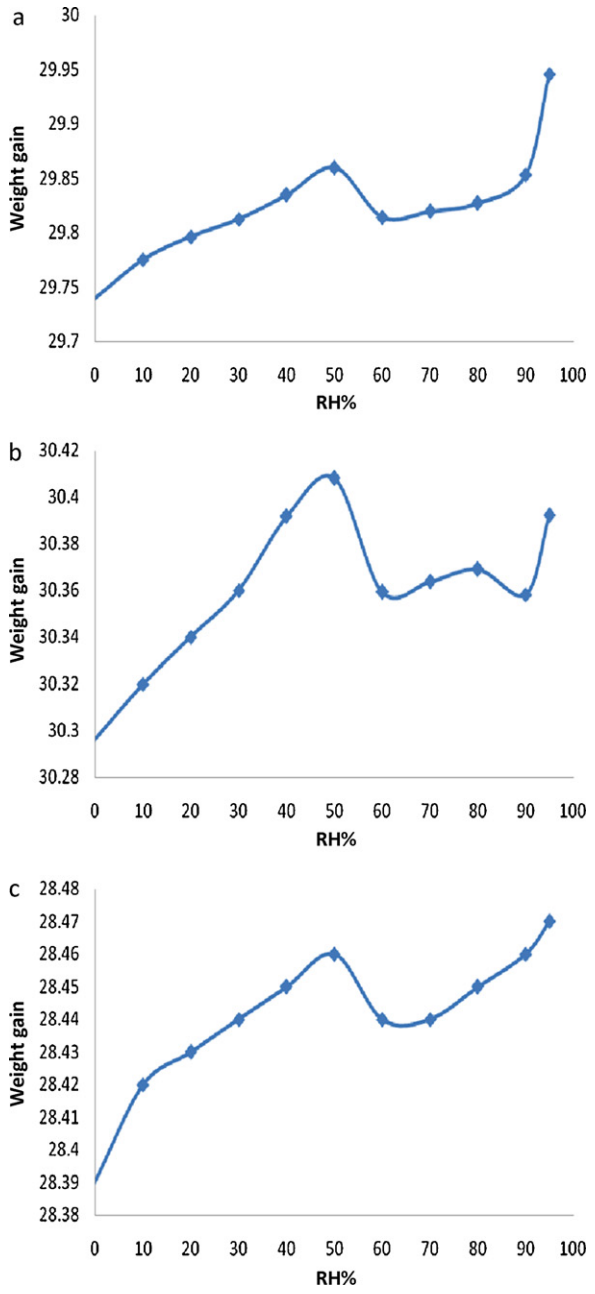

Fig. 10. Sorption data measured by DVS for (a) freshly micronised SS3-1, (b) freshly micronised SS2-1, and (c) micronised SS2-1 after four months at 25 °C.

mill chamber, which increases the number of collisons and stress events leading to greater comminution.

Injector pressure was shown to have limited influence on the particle size achieved for the different starting materials of salbutamol sulphate, with constant grinding pressure (GP). This variable was kept constant in this study since Brodka-Pfeiffer et al. (2003) have previously observed that GP markedly affects the micronisation of SS.

3.4. Surface analysis

3.4.1. Dynamic vapour sorption (DVS)

Degree of crystallinity data determined by DVS (Table 5) showed small differences in relative crystallinity for batches micronised from the two different sieve sized starting materials (50–250 μm and <20 μm), which is attributed to the brittle behaviour of SS. Batches micronised from SS2 showed low relative crystallinity (93%) compared to batches micronised from SS1 and SS3 (Table 5) when using similar processing conditions (Table 2).

This finding is thought to be due to the greater density of defects and dislocations observed for SS2 crystals, which were apparent in the starting material (see Fig. 3). Brodka-Pfeiffer et al. (2003) observed that under optimised micronisation conditions an average of 6.9% amorphous content was generated for micronised SS powders. Micronised batches of SS1 and SS3 in this study exhibited similar level of crystallinity (Table 5). Thus, these results suggest that the starting material morphology plays an important role during micronisation, particularly for crystals (SS2) with an initial higher density of dislocations. The higher dislocation density would result in a more plastically deforming material requiring increased milling residence time for particle size reduction, thereby leading to micronised product with a higher amorphous content.

In contrast, processing conditions (FR and IP) showed no notable effect on the relative percentage crystallinity for the micronised batches of SS1, SS2 and SS3.

In previous studies Ward and Schultz (1995) showed that the critical relative humidity for recrystallisation of amorphous crystallographic domains for SS is 50% RH at 60 °C, whilst Columbano et al. (2002) found that the SS recrystallised at 75% RH when the temperature was 25 °C. In this study DVS data indicated that micronised batches of salbutamol sulphate showed a recrystallisation event at 50% RH at 25 °C (Fig. 10a), as a consequence of surface disorder generated after micronisation. DVS data also revealed a double recrystallisation event for a number of micronised batches of SS2 which occurred at 50% and ~75% RH (Fig. 10b).

This interesting phenomenon is thought to be due to the presence of both bulk and surface amorphous content in the micronised SS2-1. SS2-1 initially showed double recrystallisation events immediately after micronisation (Fig. 10b). However DVS data for this batch after four months storage showed only a single recrystallisation event at 50% RH (Fig. 10c) with a decreased percentage of amorphous content from 7.0 to 4.4% (Table 5) when stored in sealed vials in desiccators (20–25% RH) at room temperature. This change is attributed to the recrystallisation of amorphous domains after four months originally located on particle surfaces, which has entrapped internal amorphous domains which were then not detected by DVS analysis on examination after storage. PXRD data of the stored sample shows scattered diffuse peaks at lower 2θ angles (Fig. 11), which indicates the presence of bulk amorphous material and emphasises that time dependent changes in amorphous salbutamol sulphate samples is a complex phenomenon (Columbano et al., 2002).

These findings also indicate that micronised drug powder may contain a mixture of crystalline, surface disorder and bulk disorder domains, for which the starting material characteristics and processing conditions have a great influence.

3.4.2. Inverse gas chromatography (IGC)

IGC data (Table 6) showed that dispersive and specific surface energies increased for the micronised batches of SS compared to the starting materials, which is consistent with the results reported by Ticehurst (1995). Starting material SS1 exhibit higher specific surface free energy (for the $CHCl_3$ probe) compared to SS2 and SS3, which can be assigned to the morphological difference observed during the DVS study for these starting materials. However micronised batch SS1-1 showed a decrease in specific free energy for $CHCl_3$ when compared with the starting SS1, which is attributed to the decreased basic surface chemistry characteristic of SS1 after micronisation. This phenomenon is explained via the increased relative surface area of (2 0 0) faces for the micronised batches of SS1 with decreased electron donating capacity (Fig. 4c), which is thought to be the cleavage plane for SS1 crystals.

Table 5
Percentage crystallinity data for the batches micronised from SS1, SS2 and SS3.

Startting material	Micronised samples code	Storage time	Relative crystallinity (%)
SS1	SS1-1	Freshly micronised	99.1 (0.2)
	SS1-1	After four months*	100.0 (0.1)
	SS1-2	Freshly micronised	98.3 (0.1)
SS2	SS2-1	Freshly micronised	93.0 (0.4)
	SS2-1	After four months*	95.6 (0.2)
	SS2-2	Freshly micronised	93.6 (0.3)
SS3	SS3-1	Freshly micronised	99.7 (0.3)
	SS3-1	After four months*	100.0 (0.1)
	SS3-2	Freshly micronised	100.0 (0.1)

* indicate the storage condition of samples at ambient temperature and 20–25%RH in desiccators in closed vials over phosphorous pentooxide.

Table 6
Dispersive and specific surface free energy for the starting and micronised batches of SS1, SS2 and SS3 (values in brackets indicate range value, where $n = 2$).

Batches	Dispersive surface energy (mJ/m^2)	Specific surface energy (kJ/mol)		
		$CHCl_3$	THF	AC
SS1	34.10 (1.12)	2.33 (0.20)	2.30 (0.09)	2.86 (0.08)
SS1-1	39.21 (2.20)	1.48 (0.07)	2.28 (0.07)	3.30 (0.07)
SS1-1 (after 4 months)	38.01 (1.31)	1.50 (0.25)	2.31 (0.08)	3.31 (0.03)
SS2	47.03 (3.90)	1.35 (0.17)	6.01 (0.17)	8.10 (0.25)
SS2-1	77.80 (4.21)	1.32 (0.10)	8.54 (0.25)	8.94 (0.13)
SS2-1 (after 4 months)	63.13 (4.51)	1.50 (0.25)	8.60 (0.21)	9.02 (0.30)
SS3	41.20 (1.60)	1.44 (0.23)	4.79 (0.16)	6.75 (0.25)
SS3-1	50.71 (1.20)	1.58 (0.14)	7.51 (0.19)	8.64 (0.12)
SS3-1 (after 4 months)	48.22 (1.12)	1.65 (0.10)	7.54 (0.14)	8.70 (0.09)

Batches micronised from the distorted plate like crystals (SS2) however showed higher dispersive and specific surface free energy than the batches micronised from SS1 and SS3 (Table 6). These crystals with a large number of defects are likely to behave more plastically during particle size reduction, leading to more disordered micronised product compared to batches micronised from SS1 and SS2. IGC data recorded after storage of four months after processing showed a marked decreased of dispersive surface free energy for micronised batches of SS2-1, with no notable changes observed for the micronised batches of SS1-1 and SS3-1 (Table 6). This effect is linked to the recrystallisation of high amount of amorphous content observed during the DVS study for micronised SS2-1 compared to SS1-1 and SS3-1 (Table 5). This finding gives support to a proposal that mechanical activation of micronised drug particles is not only dependent on the processing conditions of the microniser but also on the morphology and quality (defects and dislocations) of the starting materials.

The morphology of the starting material showed a marked impact on the dispersive surface free energy for the micronised batches of SS1, SS2 and SS3 (Table 6). Thus starting materials having higher dispersive surface free energy (SS2), typically lead to micronised materials with the highest dispersive surface free energy after processing. Increased values of dispersive surface free energy for the micronised batches of SS1, SS2 and SS3 are thought to be related to the degree of disorder generated (Fig. 11), opening of new crystalline facets with high surface energy (Heng et al., 2006) and the particle size distribution observed after micronisation (Table 4). However batches micronised from SS1 demonstrated a smaller increase in dispersive surface free energy, which is attributed to the

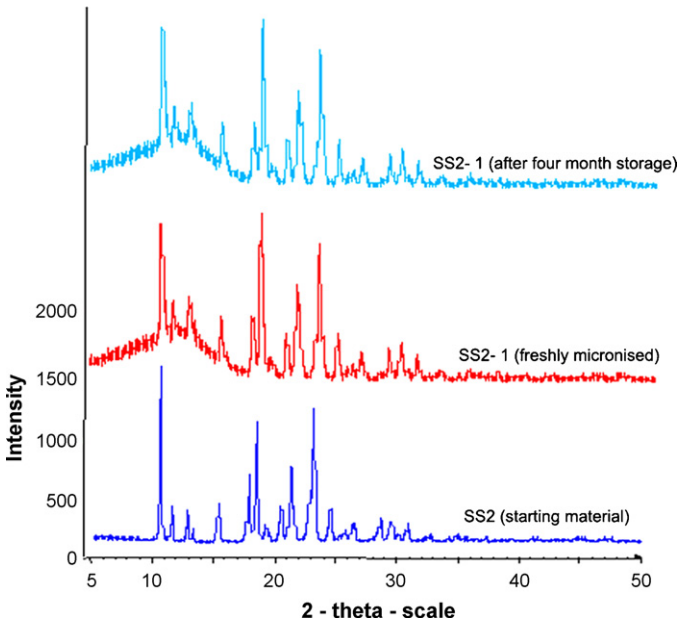

Fig. 11. PXRD data for the starting material SS2, micronised SS2-1 and micronised batch SS2-1 stored at 20–25% RH and room temperature in desiccators.

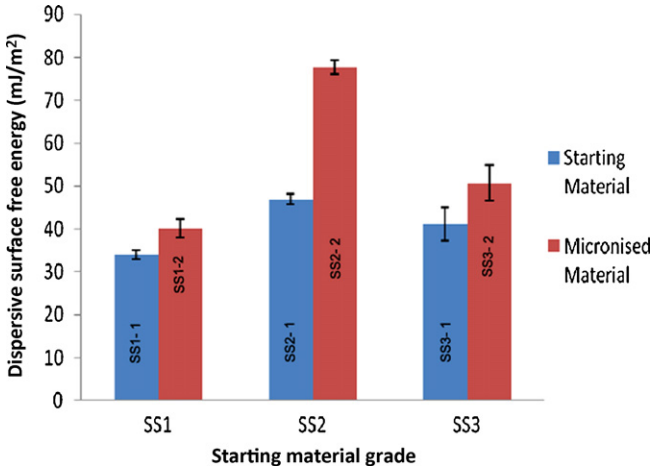

Fig. 12. Effect of starting material particle size on dispersive surface free energy observed for micronised batches of SS1, SS2 and SS3.

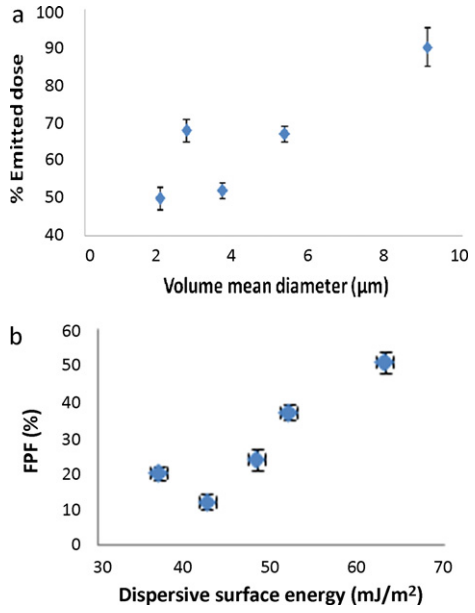

Fig. 13. Relationship between (a) volume mean diameter and % emitted dose and (b) dispersive surface energy and % FPF for micronised salbutamol sulphate.

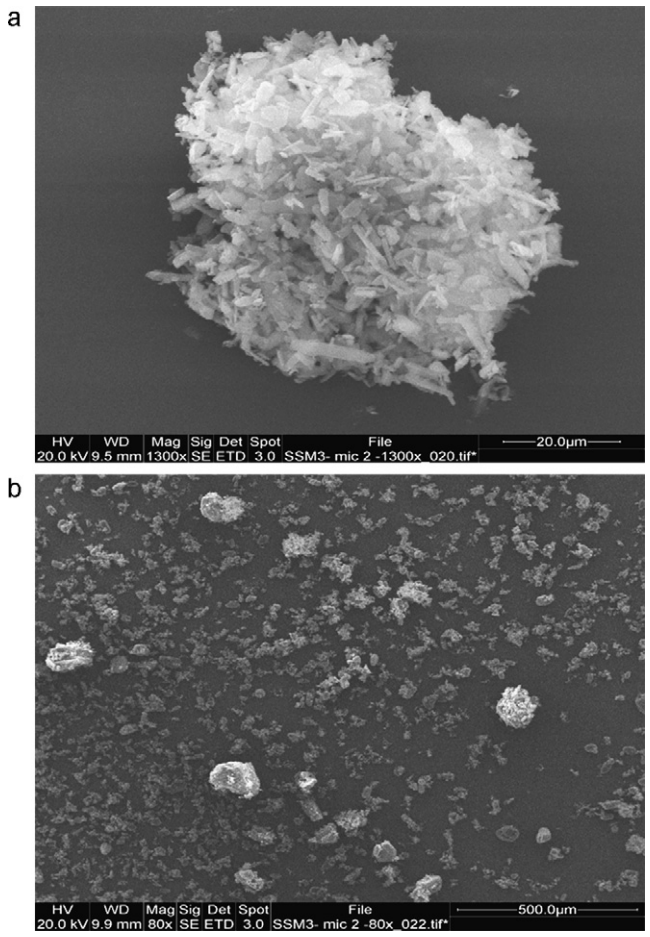

Fig. 14. SEM photomicrographs showing (a) loose aggregate of micronised salbutamol sulphate SS2-1 (magnification 1300×) and (b) SS2-1 (magnification 80×).

more brittle behaviour of this material during processing. It was hypothesised that particle size reduction for SS1 crystals is most likely occurring by brittle fragmentation via the (2 0 0) face, which has the lowest attachment energy (−61.8 kJ/mol) (Feeley, 1999). This plane is believed to be the slip and cleavage plane for this crystal, at which forces can concentrate to facilitate size reduction leading to a decrease in milling residence time (Table 6). However for SS2 and SS3 crystals the (0 0 $\bar{2}$) face is the major habit face. Therefore particle size reduction is more likely to occur by brittle fragmentation via the (0 0 $\bar{2}$) face which also has a relatively low attachment energy (−81.1 kJ/mol). Thus these results suggest that for SS crystals both (2 0 0) and (0 0 $\bar{2}$) faces can be the slip and cleavage plane (Fig. 4) due to their low attachment energies (Feeley, 1999), which is dependent on the morphology of SS crystals.

The particle size of the starting material was shown to have a marked effect on the dispersive surface free energy for the batches micronised from SS1 and SS2, whilst having no marked effect for the micronised batches of SS3 (Fig. 12). This is thought to be linked to the difficulties associated with sieving of needle like crystals of SS3. The particle size of the starting materials for SS2 prior to micronisation demonstrated a greater effect on dispersive surface free energy (Fig. 12). This phenomenon is attributed to small sized particles of SS2 containing a reduced number of defects compared to the larger sized SS2, which leads to a shortened residence time during milling and subsequent surface free energy.

Feed rate and injector pressure showed no marked effect on the dispersive surface free energy for the micronised batches of SS1, SS2 and SS3.

In contrast from Table 6, specific interactions were increased with the amphoteric probe (AC) for the micronised batches of SS, which is assigned to the presence of an increased surface area of the micronised drug powders leading to increase in the exposure of both electron donor and acceptor groups at surface. The starting material SS2 and batches micronised from SS2 and SS3 showed high specific surface free energy measured using acetone and THF, compared to batches micronised from SS1 (Table 6). These features are thought to be due to the degree of disorder and low VMD observed for micronised batches of SS2 and SS3 respectively, which is consistent with DVS data (Table 5) and particle size distribution data (Table 4). This phenomenon is most likely also due to the difference in morphology observed for these starting materials, which influences the slip direction during particle size reduction and subsequent influence on surface free energy. As mentioned above for SS1 crystals, particle size reduction is thought to occur by brittle fragmentation via (2 0 0) face, whilst for SS2 and SS3 crystals it is likely to occur via (0 0 $\bar{2}$) face (Fig. 4). These proposals are consistant with the IGC data (Table 6) observed for the micronised batches of SS1, SS2 and SS3. However high specific surface free energy for SS2 starting material is attributed to the greater number of defects and cracks observed for these materials, which exposes the polar functional groups to a greater extent.

3.4.3. *In-vitro aerosolization study*

In vitro data (Table 7) generated using the TSLI showed that a high % FPF was achieved for batches micronised from SS2 compared to batches micronised from SS1, SS3 or the micronised batches obtained from the two generic suppliers (A and B). The highest % FPF observed for SS2-1 (51%) was also higher than that was observed by Kaialy et al. (2010) (44%) using a similar flow rate (92 l/min) and DPI device (Aerolizer®).

Fig. 13a shows that the percentage emitted dose, calculated as a proportion of the recovered dose increased with higher volume mean diameter of micronised powders, which is likely to be due to improved flow characteristics for these materials.

The high value of FPF for SS2-1 is related to the marked cohesion and consequent aggregation of micronised powder produced for SS2 (Fig. 13b) giving aggregates of approximately 60–70 μm size (Fig. 14), which were characterised by high dispersive surface

Table 7
Volume mean diameter, % crystallinity, dispersive surface free energy and in vitro study data (using TSLI) of micronised batches of SS1, SS2 and SS3 after four month (values in brackets indicate standard deviation, for dispersive surface energy it indicates range value $n = 2$).

Sample	Volume mean diameter (μm) measured at 1 bar	Crystallinity (%)	Dispersive surface free energy (mJ/m^2)	FPF (%)	Emitted dose (%)
SS1-1	5.30 (0.24)	100.0(0.1)	38.01 (1.31)	20.0 (2)	67.0 (2)
SS2-1	2.70 (0.06)	95.6 (0.2)	63.13 (4.51)	51.0 (3)	68.0 (3)
SS3-1	3.65 (0.04)	100.0 (0.1)	48.22 (1.12)	24.0 (3)	50.0 (2)
Generic A	9.08 (0.26)	100.0 (0.1)	42.52 (1.51)	12.0 (2)	90.0 (6)
Generic B	2.00 (0.03)	100.0 (0.1)	51.90 (1.60)	37.0 (2)	50.0 (3)

energy from IGC data (Table 6). During delivery from the DPI device these aggregates will have experienced greater fluidization energy, a feature also observed by Kinnumen et al. (2010) using lactose blends containing high levels of fine lactose.

Price and Young (2004) also suggested that greater aerodynamic drag forces were required to aerosolize aggregated drug particles, which will initially resist dispersion until a critical force is achieved, causing them to disperse rapidly and consequently give high % FPF.

4. Conclusions

The findings detailed in the chapter indicate that crystallographic quality (cracks, defects and dislocations) and the morphology of crystals influence the micronisation behaviour of salbutamol sulphate, which can be linked to the crystallisation conditions used in their production. Further work however needs to be undertaken to understand the influence of crystallisation conditions on the morphology of SS. Results suggest that larger sized starting materials have a greater density of crystal cracks and dislocations compared to small sized starting material with similar morphology. This phenomenon has influenced the micronisation behaviour of SS crystals and subsequent quality of micronised drug particles. It was also observed that the level of processing conditions used during micronisation has a marked impact on the quality of micronised product. More specifically results indicate that batches micronised from SS3 needle like crystals demonstrate lower VMD values compared to batches micronised from SS1 and SS2. Batches micronised from SS2 exhibit reduced crystallinity and had higher surface free energy than batches micronised from SS1 and SS3, which is attributed to the greater degree of defects and dislocations of the SS2 starting material. IGC data suggest that starting SS1 materials were more basic compared to starting SS2 and SS3, which was determined using the acidic probe $CHCl_3$ (Table 3). However micronised batches of SS showed more amphoteric behaviour probably due to increased surface area to volume ratio for these drug particles, which increases the exposure of both electron donor and acceptor groups at particle surfaces. Furthermore in vitro studies have indicated that the aerosol characteristics of SS are also linked to the attributes of the starting materials. Aggregates in the size range 60–70 μm, produced from SS2 and having high density of flaws and dislocations with high dispersive surface energy (60–70 mJ/m^2) showed the optimal aerosol performance for all samples studied. It is therefore clear that optimisation of crystallisation conditions is critical to the subsequent control of micronisation and the resultant characteristics of size reduced materials, which enable the improvement of aerosol performance.

References

Brodka-Pfeiffer, K., Langguth, P., Grab, P., Hausler, H., 2003. Influence of mechanical activation on the physical stability of salbutamol sulphate. Eur. J. Pharm. Biopharm. 56, 393–400.

Blagden, N., 2004. Crystal growth mechanism. In: Encyclopedia of Supramolecular Chemistry. Marcel Dekker, Inc., 270 Madison Avenue, New York 10016.

British Pharmacopaeia, 2008. Aerodynamic Assessment of Fine Particles—Fine Particle Dose and Particle Size Distribution, vol. 4, Appendix XII C: A307, Apparatus A. Her Majesty's Stationery Office.

Columbano, A., Buckton, G., Wikeley, P., 2002. A study of the crystallisation of amorphous salbutamol sulphate using water vapour sorption and near infrared spectroscopy. Int. J. Pharm. 237, 171–178.

De Vegt, O., 2007. Jet milling from a particle perspective predicting particle fracture based on mechanical material properties. Ph.D. Thesis, University of Groningen, Netherland. ISBN: 9789090221182.

Irwin, G.R., 1948. Fracture dynamics. Trans. Am. Soc. Met. 40 (a), 147–166.

Feeley, J.C., 1999. The design and characterisation of powder particles for respiratory drug delivery. Ph.D. Thesis, University of Bradford, UK.

French, D.L., Edwards, D.A., Niven, R.W., 1996. The influence of formulation on emission, degradation and deposition of dry powders for inhalations. J. Aerosol. Sci. 27, 769–783.

Griffith, A.A., 1920. The phenomena of rupture and flow in solids. Philos. Trans. Roy. Soc. Lond., Ser. A 221, 163.

Heng, J.Y.Y., Bismarck, A., Williams, D.R., 2006. Anisotropic surface chemistry of crystalline pharmaceutical solids. AAPS Pharm. Sci. Tech. 7 (4), E1–E8.

Kaialy, W., Martin, G.P., Ticehurst, M.D., Momin, M.N., Nokhodchi, A., 2010. Enginnered mannitol as potential carrier for enhanced DPI performance. J. Pharm. Pharmcol. 62, 1432–1433.

Kinnumen, H., Shur, J., Hebbink, G., Muresan, A.S., Price, R., 2010. Lactose fluidisation properties and their relationship to dry powder inhaler performance. J. Pharm. Pharmacol. 62, 1342–1343.

Ludlam-brown, I.R., 1991. The physic-chemical and compaction properties of powders modified by alternative crystallisation conditions. Ph.D. Thesis, University of Bradford, UK.

Price, R., Young, P.M., 2004. Visualization of the crystallisation of lactose from the amorphous state. J. Pharm. Sci. 93, 155–164.

Rumpf, H., 1973. Physical aspects of comminution and new formulation of law of a law of comminution. Powder Technol. 7, 145–159.

Saxena, A., 2007. A comparative study of the surface energetic of pharmaceutical excipients by inverse gas chromatography and molecular modelling, PhD Thesis, University of Bradford, UK.

Schultz, J., Lavielle, L., 1989. Interfacial properties of carbon fiber-epoxy matrix composites. In: Lloyds, D.R., Ward, T.C., ans Schreiber, H.P. (Eds.), Inverse Gas Chromatography ACS Symposium Series 391, Washington. , pp. 185–202.

Storey, R.A., 1997. The nucleation, growth and solid state properties of particulate pharmaceuticals. Ph.D. Thesis, University of Bradford, UK.

Ticehurst, M.D., 1995. Characterisation of surface energetics of pharmaceutical powders by inverse gas chromatography. Ph.D. Thesis, University of Bradford, UK.

Vogel, L., Peukert, W., 2003. Breakage behaviour of different materials-construction of a mastercurve for the breakage probability. Powder Technol. 129, 101–110.

Ward, G.H., Schultz, R.K., 1995. Process induced crystallinity changes in albuterol sulfate and its effect on powder physical stability. Pharm. Res. 12, 773–779.

Zanen, P., Go, L.T., Lammers, J.J.W., 1995. The optimal particle size for parasympatholytic aerosols in mild asthmatics. Int. J Pharm. 114, 111–115.